JOURNAL OF MATERIALS SCIENCE 21 (1986) 3116–3124

On the applicability of linear elastic fracture mechanics to environmental stress cracking of low-density polyethylene

KOKSAL TONYALI, HUGH R. BROWN*
Department of Macromolecular Science, Case Western Reserve University, Clevelend, Ohio 44106, USA

The primary aim of this work was to re-examine the range of applicability of linear elastic fracture mechanics (LEFM) to environmental stress cracking of low-density polyethylene. By use of a number of specimen types and a range of specimen dimensions and loads it is shown that the K_I–$\dot{c}$ relationship is unique only at low K_Is. The material studied showed a region of constant crack velocity which was not caused by plasticity effects or the failure of LEFM. However, crack arrest, which occurred at high K_Is or loads, was shown to be caused by ductile yielding causing the crack to blunt.

1. Introduction

The development of understanding of environmental stress cracking (ESC) of polyethylene has been limited by the fact that neither the mechanics nor the physical chemistry of the situation are simple. The majority of work published has been based on time-to-fail experiments using either constant load or constant deformation tests. Unfortunately, this type of test is not straightforward to interpret as the mode of cracking changes during the crack propagation so a single time-to-fail need not be very informative.

As is the case in many areas of fracture, the situation has been improved by the application of linear elastic fracture mechanics (LEFM) to the problem, first done by Williams and co-workers [1, 2]. They found, perhaps surprisingly considering the viscoelastic nature of polyethylene, that in general the crack growth rate ($\dot{c}$) depended only on the stress intensity factor (K_I), e.g. a unique K_I–$\dot{c}$ relationship existed. They did, however, suggest that at high c/W (where c is the crack length and W is the specimen width) and high loads, this relationship begins to fail.

The unique nature of the K_I–$\dot{c}$ relation was confirmed by Bandyopadhyay and Brown [3] and Chan and Williams [4]. The concepts of LEFM have also been used to a more limited extent by Bubeck [5] who studied time-to-failure as a function of initial K_I.

Williams and Marshall [6] proposed that there exist three regions in a K_I–$\dot{c}$ plot, designated regions I, II and III. They suggested that these regions were controlled by relaxation processes, hydrodynamic flow properties of the environment, and failure properties of the polymer in air, respectively.

Bandyopadhyay and Brown [7] and Belcher [8] also found three regions which they interpreted in a similar way. They found, however, that in region II the crack speed was independent of K_I and that, in LDPE, region III normally shows crack arrest as the materials are ductile in air at the relevant K_I values. Chan and Williams [4] have also found a region where the crack speed is independent of K_I and ascribed it to crack blunting effects.

The aim of this work was to re-examine the application of LEFM to environmental stress cracking of polyethylene using a number of test variables such as different specimen geometries, load levels, specimen dimensions and initial crack length. Also, the three different regions of crack growth were studied separately and the results compared with existing models.

2. Experimental details

2.1. Materials

The low-density polyethylene used in the experiments was produced by Dow Chemical Company, USA. The specifications of the material (Dow polyethylene 681) are: melt flow index 0.22, and density 0.918 g cm^{-3}.

A 10% (vol/vol) detergent solution was used as an environment. The detergent (Igepal CO-630) was obtained from GAF Corporation, USA.

2.2. Sample preparation

2.2.1. Sheet preparation

The polyethylene was obtained in the form of beads and pressed into a sheet between the steel plates using a compression moulding apparatus. The temperature and the time of the moulding were 180° C and 20 min, respectively. The load exerted by the press was 40 000 lbf(177.9 × 10^3 N) and was released at the end of the moulding time. Then the sheet was air cooled to the room temperature between the plates.

The moulded sheets had dimensions of 150 mm × 150 mm with a range of thicknesses up to 5 mm. The properties of the sheets are shown in Table I.

*Present address: IBM San Jose Research Laboratory, Mail Code K 91/282, 5600 Cottle Road, San Jose, California 95193, USA.

0022–2461/86 $03.00 + .12

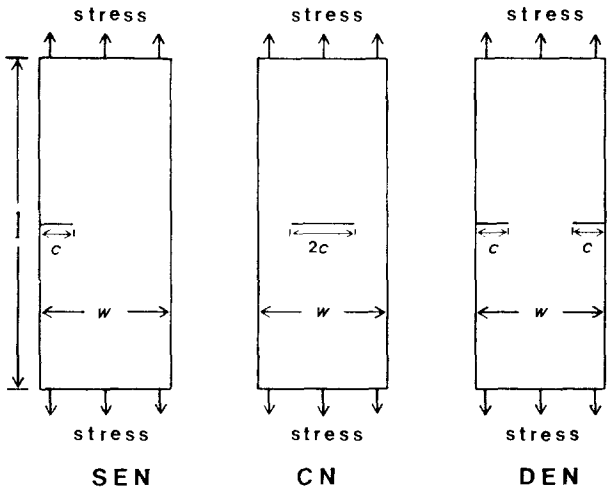

Figure 1 Three different specimen geometries used in the experiments: Singe edge-notched (SEN), centre notched (CN) and double edge-notched (DEN) specimens.

2.2.2. Specimen preparation

The specimens which were cut from the moulded sheets using a razor blade were 140 mm long and in a range of thicknesses and widths depending on the test conditions of ESC experiments which will be described later. Also a notch was introduced to the specimens using the razor blade.

2.3. Environmental stress-cracking tests

2.3.1. Experimental apparatus

An environmental stress-cracking test rig was designed and built to conduct crack propagation tests. The environmental liquids were held in glass cells mounted on the lower sample grip so that only small amounts (approximately 70 cm^3) of liquid need be used. A constant load was applied to the specimens and the crack length was monitored photographically. The crack length was measured from the film negatives with an accuracy of 0.01 mm. Unless otherwise stated tests were performed at 22° C.

2.3.2. Specimen geometries

Three different specimen shapes were used in these experiments. These, shown in Fig. 1, were single edge-notched (SEN), centre notched (CN) and double edge-notched (DEN). K_I was obtained using the standard relationship

$$K_I = Y\sigma(\pi c)^{1/2} \quad (1)$$

where Y was obtained for the three geometries from the work of Tada *et al.* [9].

TABLE I Properties of the moulded low-density polyethylene sheet

Young's modulus (MPa)	Yield stress (MPa)	Yield strain	Ultimate stress (MPa)	Ultimate strain
175	11.4	0.30	16.1	5.52

2.3.3. Data analysis

To obtain K_I–$\dot{c}$ plots the crack length (c) against time (t) curves were fitted using spline functions and differentiated to obtain the crack velocity. Data points are shown at each crack length measurement position.

2.4. Fracture surface analysis

2.4.1. Optical microscopic studies

The fracture surfaces were examined under a Zeiss microscope and dark-field pictures were taken when required.

2.4.2. Scanning electron microscopic studies

The fracture surfaces were coated with Au–Pd using Polaron SEM Coating System. The specimens were cooled down at interval times during the coating procedure in order to prevent the heating damage on the fracture surface. These specimens were examined in the scanning electron microscopes, namely, Cambridge S4-10 Stereoscan microscope and Jeol JSM-35CF microscope.

3. Results and discussion

3.1. Application of fracture mechanics to ESC

3.1.1. Comparison between the results of SEN, CN and DEN specimens

The K_I–$\dot{c}$ plots for CN, DEN and SEN specimens are compared in Fig. 2. The specimen dimensions were 120 mm × 40 mm × 1.35 mm with a nominal applied stress 0.70 MPa. It is clear from the K_I–$\dot{c}$ plot that the agreement between the different specimen geometries

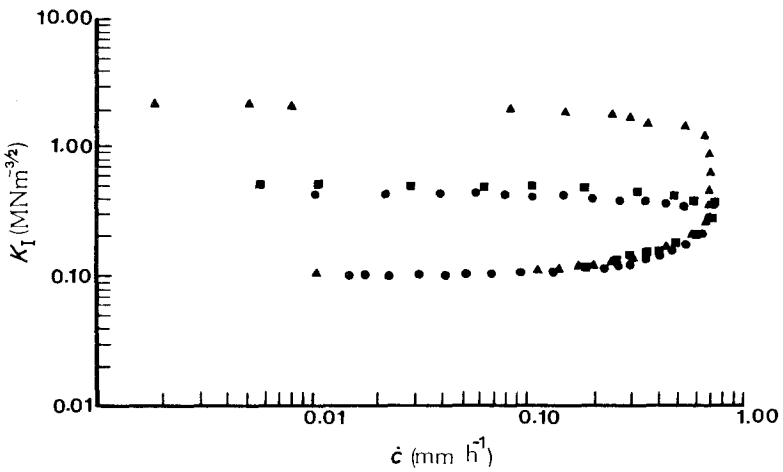

Figure 2 Comparison of the K_I–$\dot{c}$ plots of the CN, DEN and SEN specimens. ● CN, ■ DEN, ▲ SEN.

is not good. There is a large difference between the results of the SEN and CN or DEN specimens. All three geometries agree well at low K_I and the symmetric geometries, DEN and CN agree well over the whole K_I range. However, the results at higher K_I from the asymmetric SEN specimen diverge from those obtained from the symmetric specimens.

The three regions of crack growth are seen clearly in this figure. There is apparently a critical K_I below which no crack propagation occurs, this is normally called K_{ISCC} and is approximately $0.1\,MN\,m^{-3/2}$. Region I is found between K_{ISCC} and K_I where the speed becomes constant. Region II is the constant speed region and region III the "crack arrest region" where the crack decelerates and blunts. Region II is particularly important as most damage is introduced into the material at this stage. It is region III that differs so much between the symmetric and asymmetric samples. For example, crack arrest starts to occur at about $K_I = 0.4\,MN\,m^{-3/2}$ for the CN and DEN samples whereas it begins at $K_I = 2.0\,MN\,m^{-3/2}$ approximately for the SEN samples.

After crack arrest, which occurred when the crack tip blunted, the net cross-sectional areas were measured for the different geometries and the net stress was calculated for each of them. The results are: $\sigma_{SEN} = 3.65\,MPa$, $\sigma_{CN} = 10.62\,MPa$, $\sigma_{DEN} = 11.66\,MPa$. The yield stress of the material is 11.40 MPa. From these results it is clear that in the CN and DEN specimens crack arrest occurs when the net section stress reaches the yield stress. However, the net stress for the SEN samples is quite small compared to the CN and DEN samples. It will be shown later that this effect may be attributed to the bending of the SEN samples at high c/W ratios which increases the stress at the crack tip. Hence, although the yield stress is not reached over the whole section, the crack tip blunts because local yielding is caused by the bending stress. The bending effect will be discussed later in more detail.

The fracture surface studies were carried out at the three regions in the scanning electron microscope. Fig. 3 shows that the fracture surface appearance is the same at the same region for the three different geometries. Hence in regions I and III the fracture surface appearance correlates with crack velocity rather than nominal K_I. In region II the velocity is constant and the roughness increases with increasing K_I, as has been observed before [10]. The micrographs are similar at the beginning of region II ($K_I = 0.25\,MN\,m^{-3/2}$, see Fig. 3b). Towards the end of region II, the micrographs

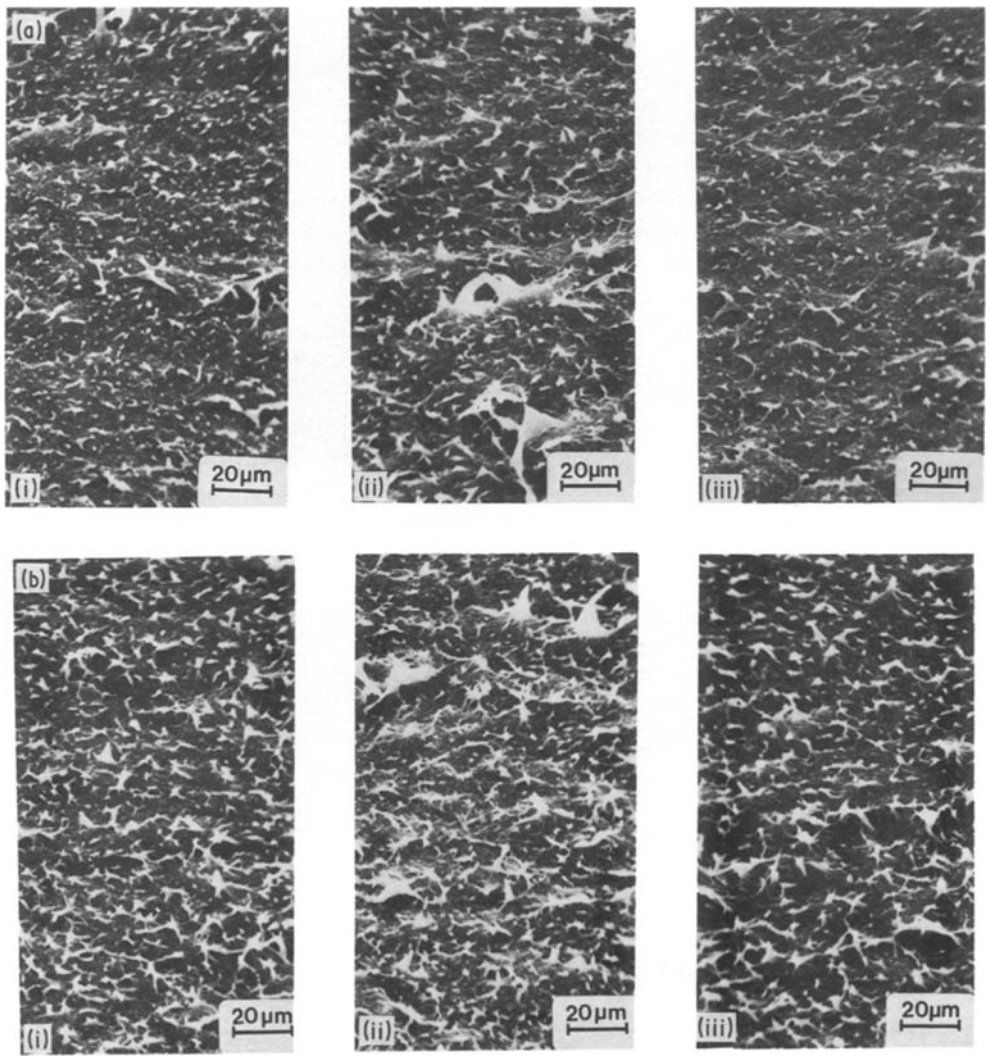

Figure 3 Comparison of scanning electron micrographs of the (i) CN, (ii) DEN and (iii) SEN samples in (a) region I, (b) at the start of region II, (c) in region II, and (d) in region III. (a) $K_I = 0.10\,MN\,m^{-3/2}$; (b) $K_I = 0.25\,MN\,m^{-3/2}$; (c) (i) and (ii) $K_I = 0.4\,MN\,m^{-3/2}$, (iii) $K_I = 1.0\,MN\,m^{-3/2}$; (d) (i) and (ii) $K_I = 0.5\,MN\,m^{-3/2}$, (iii) $K_I = 2.0\,MN\,m^{-3/2}$.

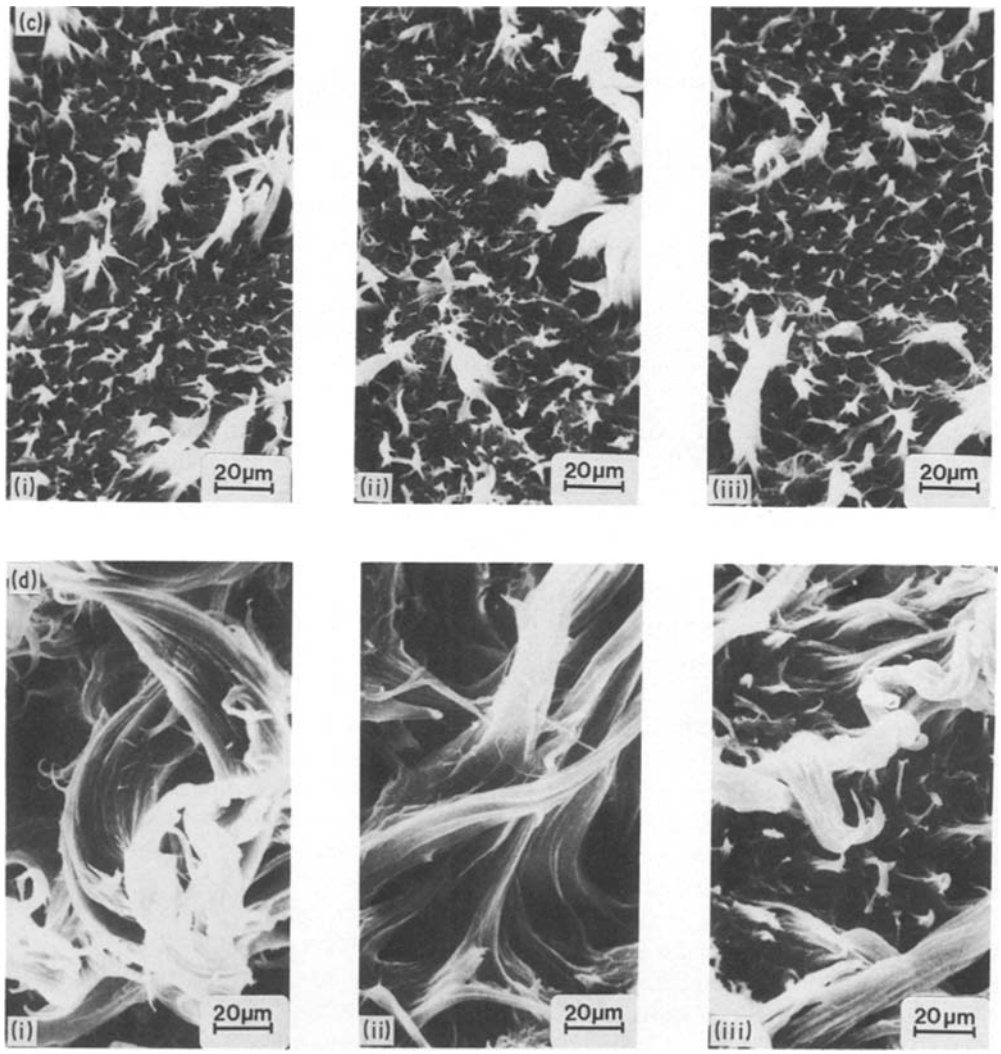

Figure 3 Continued.

are similar but K_I values are not the same (i.e. $K_I = 0.4\,MN\,m^{-3/2}$ for the CN and DEN samples and $K_I = 1.0\,MN\,m^{-3/2}$ for the SEN samples, see Fig. 3c).

3.1.2. Effect of initial stress levels on K_I against $\dot{c}$ plots

A number of tests were carried out to study the effect of different remote stress levels on the stress cracking of polyethylene. The effect is shown in Fig. 4. The tests were carried out at the nominal stress of 0.70, 1.18, 1.67 and 2.17 MPa with specimen dimensions of 120 mm × 40 mm × 1.35 mm. Also, another experiment was conducted at a stress level of 2.80 MPa where the crack arrested very quickly and branching was observed at the crack tip as shown in Fig. 5. However, in this material the crack growth rate was very slow once the branches were formed unlike the situation observed in previous work [10]. It was observed that crack branching took place when the tip of the crack blunted.

Returning to Fig. 4, it is clear that as the stress level increased the K_I value for crack arrest was found to

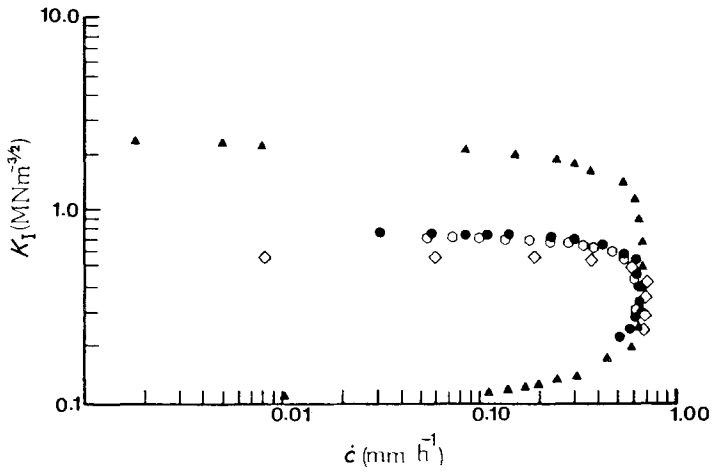

Figure 4 Effect of stress levels on the K_I–$\dot{c}$ plots. ▲ 0.70 MPa, ● 1.18 MPa, ○ 1.67 MPa, ◇ 2.17 MPa.

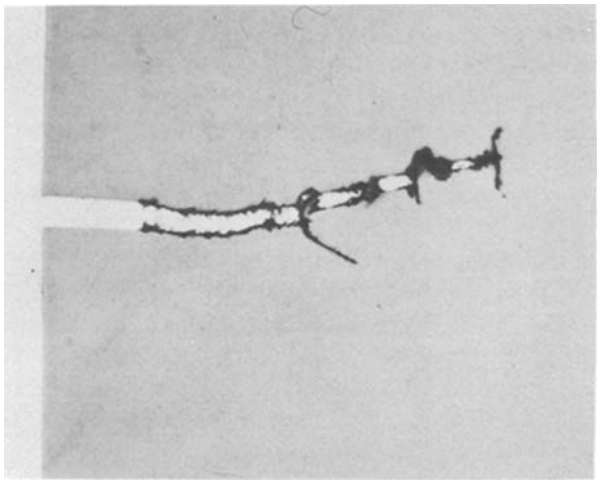

Figure 5 Crack branching after crack tip blunting.

decrease. The decrease was from $K_I = 2.3\,MN\,m^{-3/2}$ for 0.70 MPa stress level to $K_I = 0.6\,MN\,m^{-3/2}$ for 2.17 MPa stress level. The net section stress, however, was increasing from 3.65 to 6.30 MPa as the crack length at blunting became shorter and the bending effect decreased.

3.1.3. Effect of specimen width and initial crack size on the K_I–$\dot{c}$ plots

The result of an examination of the specimen width effect on the K_I–$\dot{c}$ plot is shown in Fig. 6. The specimens had a thickness of 1.35 mm and length of 120 mm with the stress level of 0.70 MPa. It can be seen from Fig. 6 that the change of the specimen width did not affect the results.

The effect of the initial crack size on the K_I–$\dot{c}$ plots was also investigated using the initial crack sizes of 4.8 and 12.5 mm. The results are shown in Fig. 7. The experimental conditions were the same as in the width studies. Fig. 7 reveals that the change in crack size does not affect the results.

3.1.4. Effect of specimen thickness on the K_I–$\dot{c}$ plots

The specimen thickness plays a large role in determining the fracture toughness of material. The effect was examined using the specimen thicknesses of 1.35, 2.55 and 3.96 mm all loaded to the same nominal stress. The effect of the thickness change is shown in Fig. 8. The curves superimposed on each other over the crack initiation and propagation regions. The K_I values for the crack arrest, however, varied a small amount at the crack deceleration region. This variation of the transition to region III with sample thickness implies that the yielding process is to some extent through-thickness and that the conditions in region II must be plane strain. Failure normally ceases to be plane strain when the plane stress (surface) plasic zone at the crack tip becomes comparable in size to the specimen thickness. In the small scale yielding approximation the plastic zone radius (r_p) is often given by

$$r_p = \frac{1}{2\pi}\left(\frac{K_I}{\sigma_y}\right)^2 \tag{2}$$

The ASTM Standard condition for specimen thickness

$$B \geqslant 2.5\left(\frac{K_I}{\sigma_y}\right)^2 \tag{3}$$

which works well for polymers [11], implies that $B \geqslant 16r_p$. For 1.35 mm samples the ASTM plane strain criterion fails when $K_I \geqslant 3 \times 10^5\,N\,m^{-3/2}$, this value is near the beginning of the constant crack speed region, approximately where the symmetric and asymmetric samples begin to diverge.

3.1.5. Crack opening displacement measurements

The crack opening displacements (COD) were measured photographically for the CN, DEN and SEN specimens and also calculated theoretically. The crack opening displacement (b) at the edges or centre depending on the specimen geometry is given as

$$b = \frac{4\sigma c(1-\nu)}{E} V_1(c/w) \tag{4}$$

where σ is the applied stress, c is the crack length, E is the Young's modulus, ν is the Poisson's ratio and $V_1(c/w)$ is the geometric factor. $V_1(c/w)$ can be found in Tada *et al.* [9].

The plot of the calculated COD (b_c) against the measured COD (b_m) can be seen in Fig. 9. It is interesting to note that initially the COD of the three different geometries follow a single line which has a slope of 1.0. However, the line separates into two

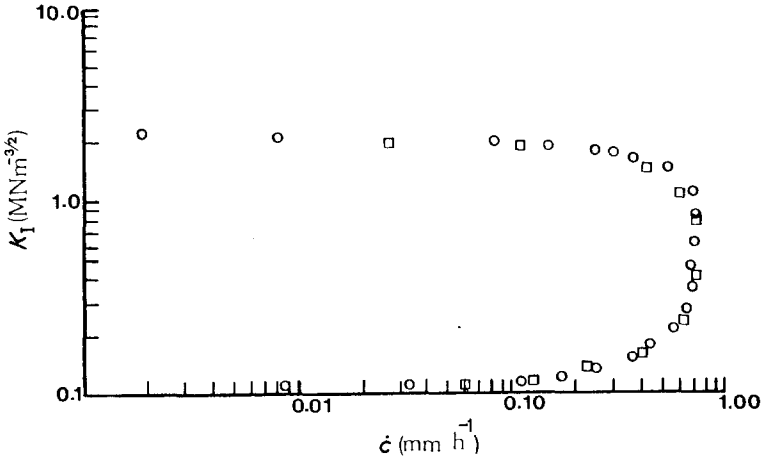

Figure 6 Effect of specimen width on the K_I–$\dot{c}$ plots. o 40 mm, □ 20 mm.

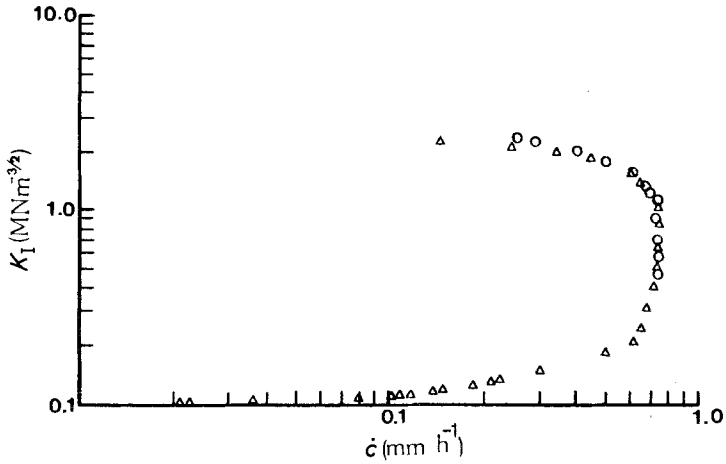

Figure 7 Effect of initial crack size on the K_I–$\dot{c}$ plots. △ 4.8 mm, ○ 12.5 mm.

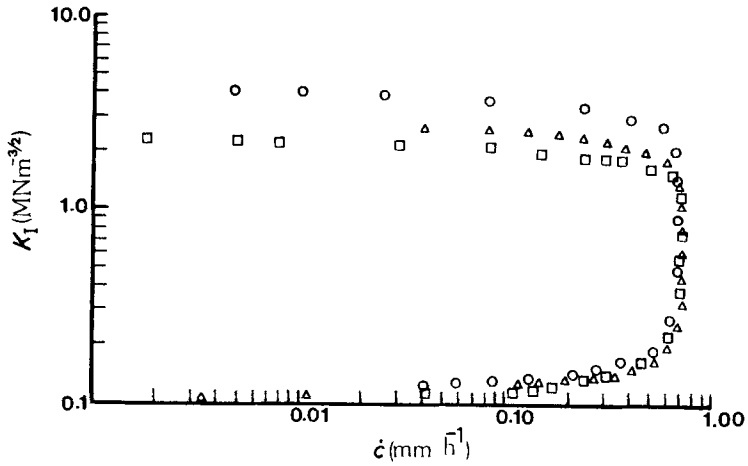

Figure 8 Effect of speciment thickness on the K_I–$\dot{c}$ plots. □ 1.35 mm, △ 2.55 mm, ○ 3.96 mm.

different curves, one is for the SEN specimens and the other for the CN and DEN specimens as the COD becomes larger. The deviation starts at $K_I = 3.0$ MN m$^{-3/2}$ approximately the value at which LEFM ceases to apply.

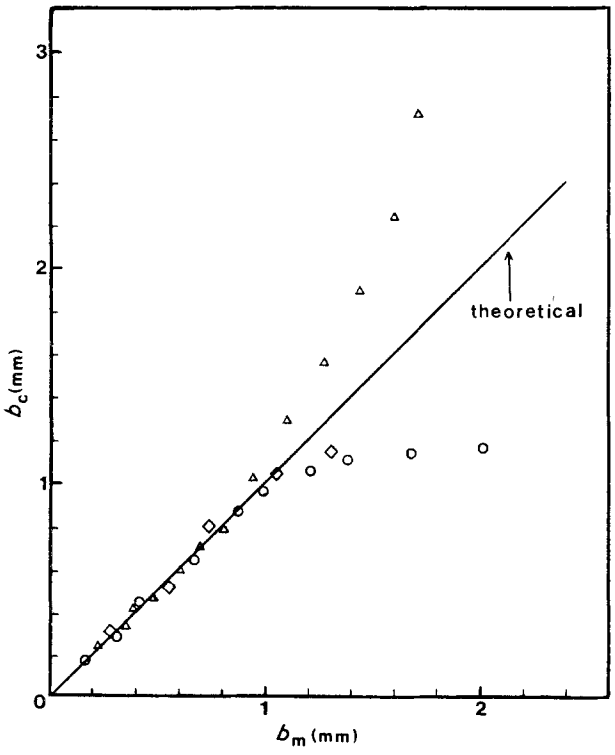

Figure 9 Comparison between the measured (b_m) and calculated (b_c) crack opening displacements. △ SEN, ◇ DEN, ○ CN.

It can be seen that the rapid deviation of the crack propagation results for the two basic specimen types is caused by opposite effects of a significant plastic zone on the COD. In the asymmetric samples the plastic zone enhances a hinge effect and increases the COD whereas in the symmetric sample the plastic zone tends to even the stress out over the unbroken ligament, decreasing the bending in that area and hence the COD.

3.2. The three regions of crack propagation

Williams and Marshall [6, 11] have proposed that ESC crack propagation can be considered in three regions corresponding the three different types of behaviour. These three regions will be considered here.

3.2.1. Region I

Williams proposed that in this region the fluid can keep up with the crack tip and that the failure was relaxation controlled. From this he predicted that

$$K_I \propto (\dot{c})^{0.1} \quad (5)$$

Both the results in this paper and those published earlier [12] do not give a straight line on a log–log plot so do not agree with this suggestion. In addition it would appear from these results that a minimum K_I for crack propagation probably exists.

The fracture surface was studied at this region. It appeared brittle-like with very small fibrils in the surface, probably the result of the drawing of the material occurring during the crack growth process (see Fig. 10).

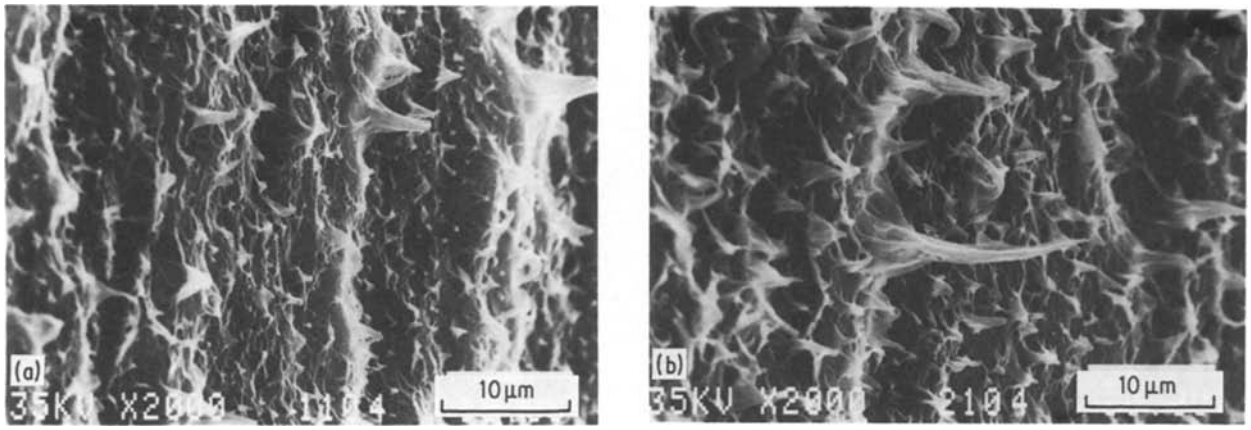

Figure 10 Scanning electron micrographs of the SEN specimen in region I. (a) $K_I = 0.1\,MN\,m^{-3/2}$, (b) $K_I = 0.2\,MN\,m^{-3/2}$.

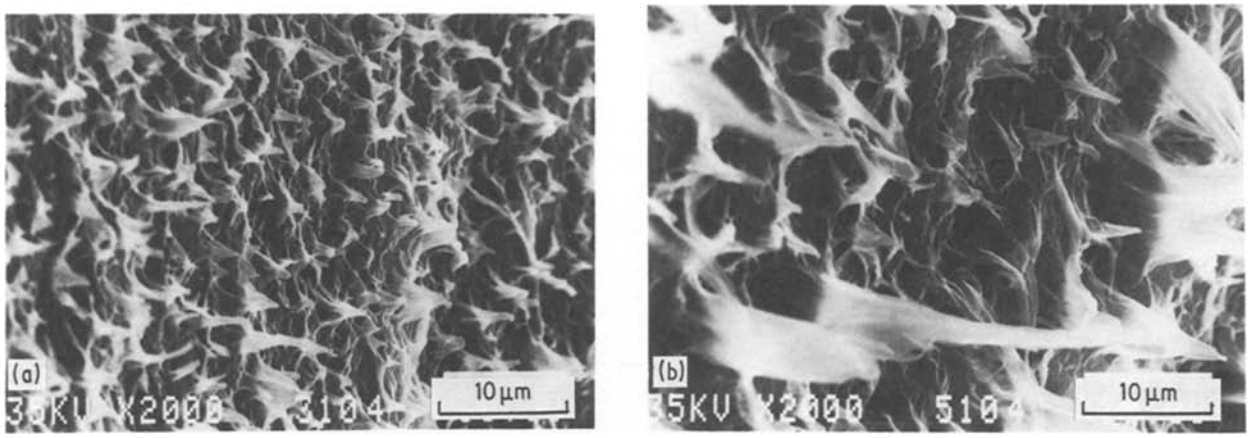

Figure 11 Scanning electron micrographs of the SEN specimen in region II. (a) $K_I = 0.4\,MN\,m^{-3/2}$, (b) $K_I = 0.8\,MN\,m^{-3/2}$.

3.2.2. Region II

Williams suggested that the second region of crack propagation was flow controlled and that the plot of log (K_I) against log ($\dot{c}$) should give a slope of 0.5 [6] or infinity [11]. In this work, in agreement with previous work [12], we found that Region II is a constant crack speed region (infinite slope). In a recent paper, Chan and Williams [4] made a similar observation in the fracture of high-density polyethylene in 2% detergent solution. It is not clear that this region is flow controlled; however, evidence will be presented in another paper [13] on the effect of detergent concentration on the crack velocity which strongly argues against flow control.

Chan and Williams also suggested that the high slopes ($> \frac{1}{2}$) of log K_I–log $\dot{c}$ curves were caused, at least in HDPE, by crack blunting effects. In previous work using a range of LDPEs of similar density but different molecular weight it was shown that K_I for the transition from regions I to II increased with increasing molecular weight and all molecular weights showed constant crack speed in region II. Blunting effects would be expected to be controlled mainly by the modulus and yield stress of the materials so to occur at a similar K_I in all these materials. It seems unlikely then that either the region I to region II transition or the existence of a constant crack speed in region II are caused by blunting in LDPE.

An example of the fracture surface is shown in Fig. 11. The micrograph is taken at $K_I = 0.4$ and

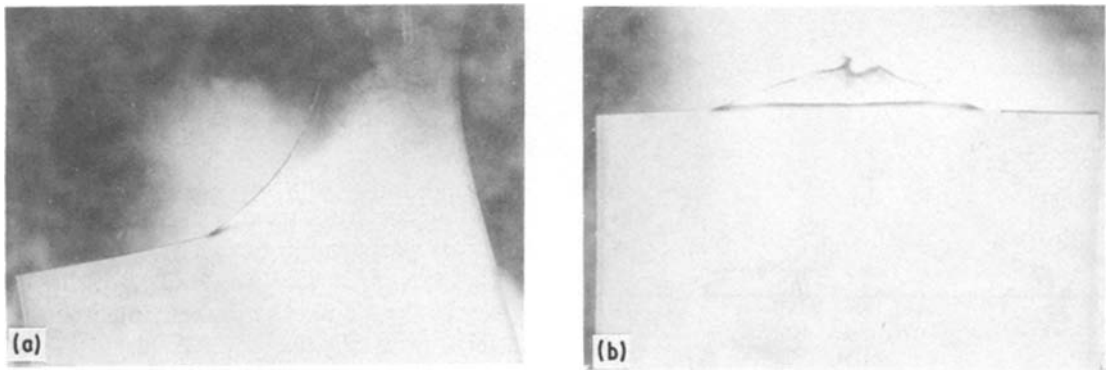

Figure 12 Deformation of the (a) SEN and (b) DEN specimens when loaded in air.

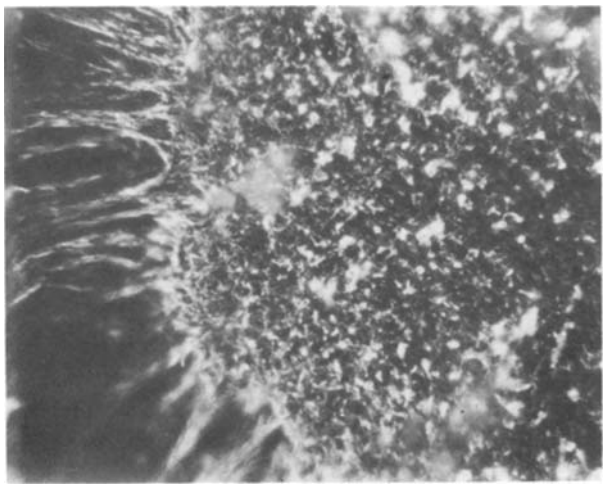

Figure 13 Appearance of crack tip when blunted (dark-field picture, × 108).

$0.8\,MN\,m^{-3/2}$. The roughness of the surface has increased as K_I increased and the fibrils have become thicker.

3.2.3. Region III

Williams [11] proposed that the constant crack speed region ends when the stresses become large enough that cracking occurs as in air. In brittle high-density polyethylenes, as stress intensity factor is increased, the crack speed increases very rapidly at the end of region II. However, Bandyopadhyay and Brown [7] and Belcher [8] have shown for low-density polyethylenes that crack deceleration occurs at the end of region II. This behaviour is also observed in this work. As the end of region II is reached, the crack tip loses its sharpness and finally becomes circular in shape which means the loss of stress concentration at the crack tip taking place. Earlier in this paper, it was suggested that, in symmetric specimens, the crack tip blunting occurs when the stress level is about the yield stress of the material. To confirm this suggestion, the CN, DEN and SEN specimens were tested in air. The specimens for each geometry had a thickness of 1.35 mm, a width of 30 mm, and different initial crack sizes to examine the crack size dependence. The samples were loaded gradually until they showed yielding at the crack tip and the loads were recorded. The comparison of the results with ESC tests are presented in Table II. It seems from these results that yielding takes place at the crack tip when it arrests. As explained earlier, although the stress is lower than yield stress for SEN samples, crack tip yielding occurs. This may be due to bending which causes extra stress concentration at the crack tip. The results in Table II show that the measured values are very close to the yield stress except in the SEN samples. The crack tip became thinner as loading increased in the SEN samples and finally it yielded and drawing took place, but no separation of the surfaces into two halves was observed (see Fig. 12). However, for the CN and DEN samples, yielding took place at a higher stress, drawing similar to that occurring in the SEN samples was not observed, and finally the separation of the two surfaces occurred. Because the material is tough, the cracks did not grow at all, but the crack tip geometry changed from a sharp tip to a circular one prior to yielding in all experiments. The initial crack sizes did not greatly affect the results.

TABLE II Comparison of net section stresses between the ESC and air tests when crack tip blunted

Environment	Stress (MPa)		
	SEN	CN	DEN
10% Detergent	3.65	10.65	11.66
Air	4.67	9.40	9.50

The above results suggest that the crack grows until the stress is high enough to cause gross yield at the crack tip. Once this stress level is attained the crack grows in a ductile manner. The stress–strain curve showed strain hardening at high extensions. Therefore, hardening may also be taking place at the crack tip at blunting. Anderton and Treloar [14] have shown that the orientation of polyethylenes causes a fracture toughness increase in the direction transverse to the orientation and the reverse effect in the parallel direction. In fact they stated that it was not possible to propagate the crack in the transverse direction. Doll and Plajer [15], Gaube [16], Heiss *et al.* [17], and Hojo and Thai [18] also observed this effect. Therefore, the orientation and strain hardening may be taking place at the crack tip when crack blunting occurs. This will require a higher K_I for crack to start growing again.

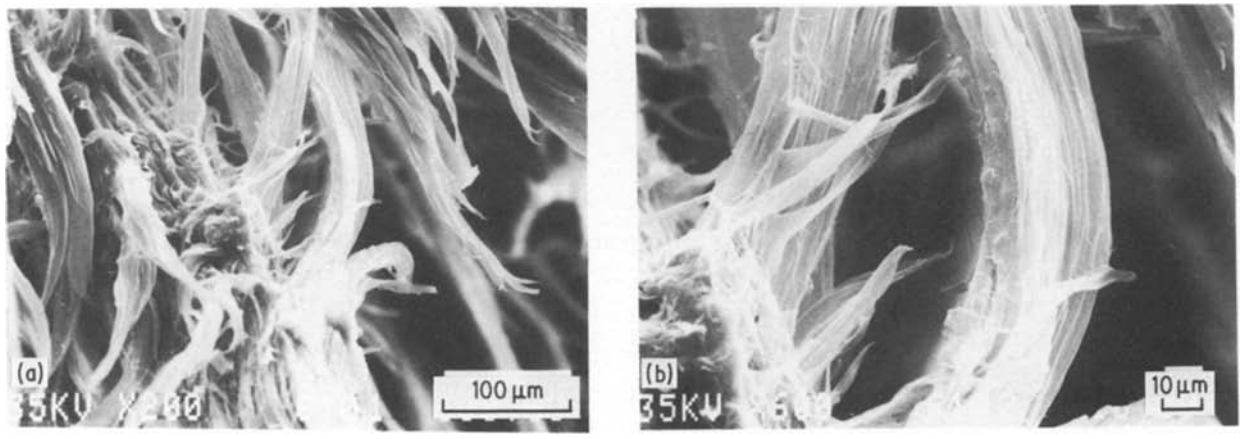

Figure 14 Scanning electron micrographs of the SEN specimen in region III. $K_I = 2.0\,MN\,m^{-3/2}$.

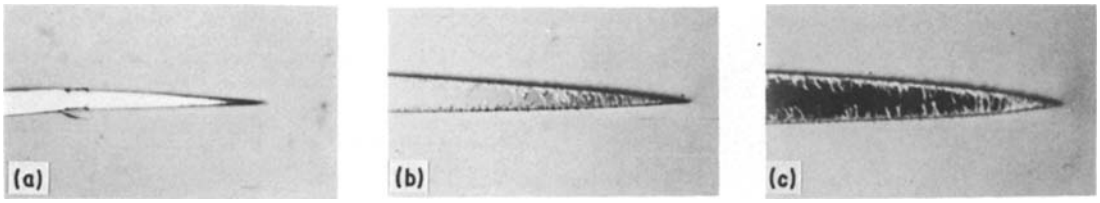

Figure 15 Crack tip pictures at different K_I values. (a) $K_I = 0.1\,MN\,m^{-3/2}$, (b) $K_I = 0.8\,MN\,m^{-3/2}$, (c) $K_I = 2.0\,MN\,m^{-3/2}$.

The fracture surfaces at the crack deceleration region were examined in the optical and scanning electron microscopes. The micrographs are shown in Figs 13 and 14. It is evident that yielding takes place at the crack tip. Fig. 14 shows that the size and amount of the fibrils have become very large and drawing has occurred at the crack tip. During the crack propagation experiments it was possible to observe thin fibrils on the surface. These fibrils became thicker as K_I increased. Also there were fibrils at the sides of the fracture surface because of the plane stress condition occurring there (Fig. 15). A comparison of Fig. 14 with Figs 10 and 11 shows that the surface is very rough in Fig. 14. This may be another reason why crack growth decelerates when drawing and yielding start to occur in large amounts.

4. Conclusion

The range of application of linear elastic fracture mechanics to the environmental stress cracking of low-density polyethylene has been re-examined. The most critical test was found to be the comparison of the results from asymmetric (SEN) specimens with those from symmetric (CN and DEN) ones. Fracture mechanics applies in region I and just into region II in the system studied here and limiting K_I agrees well with the normal published criteria.

It was proposed that the crack deceleration region occurred because of the large scale yielding at the crack tip and was controlled by the mechanical properties of the material. This was also confirmed by air tests. A substantial amount of ductile behaviour was observed on the fracture surface. When there was no bending, blunting occurred when the net section stress equalled the yield stress. The specimen width and the initial crack length did not affect the behaviour.

Acknowledgement

The financial support is provided through ARO no. DAAG29-82K-0174.

References

1. G. P. MARSHALL, L. E. CULVER and J. G. WILLIAMS, *Plastics and Polymers* **38** (1970) 95.
2. G. P. MARSHALL, N. H. LINKINS, L. E. CULVER and J. G. WILLIAMS, *SPE J.* **28** (1972) 26.
3. S. BANDYOPADHYAY and H. R. BROWN, *Polymer* **22** (1981) 245.
4. M. K. V. CHAN and J. G. WILLIAMS, *ibid.* **24** (1983) 234.
5. R. A. BUBECK, *ibid.* **22** (1981) 682.
6. J. G. WILLIAMS and G. P. MARSHALL, *Proc. R. Soc.* **A342** (1975) 55.
7. S. BANDYOPADHYAY and H. R. BROWN, *Int. J. Fract.* **15** (1979) R175.
8. J. BELCHER, MSc thesis, Monash University, Australia (1981).
9. H. TADA, P. C. PARIS and G. R. IRWIN, "The Stress Analysis of Cracks Handbook" (Del Research, Hellerton, Pennsylvania, 1973).
10. J. BELCHER and H. R. BROWN, *J. Mater. Sci.* **21** (1986) 717.
11. J. G. WILLIAMS, *Adv. Polym. Sci.* **27** (1978) 67.
12. S. BANDYOPADHYAY and H. R. BROWN, *J. Polym. Sci. Polym. Phys. Ed.* **19** (1981) 749.
13. K. TONYALI and H. R. BROWN, *J. Mater. Sci.*, to be published.
14. G. E. ANDERTON and L. R. G. TRELOAR, *J. Mater. Sci.* **6** (1971) 562.
15. H. DOLL and O. PLAJER, *Kunststoffe* **51** (1961) 358.
16. E. GAUBE, *ibid.* **49** (1959) 446.
17. J. H. HEISS, V. L. LANZA and W. M. MARTIN, *Wire and Wire Products* **34** (1959) 592.
18. H. HOJO and G. M. THAI, *J. Macromol. Sci. Phys.* **B19**(4) (1981) 589.

Received 14 August
and accepted 23 October 1985